# Characterization of nitrogen-containing adsorbates and reactants on porous catalysts by $^{14/15}$N solid-state NMR

***Spectroscopic background:*** $^{14}$N and $^{15}$N nuclei have spins of $I = 1$ and $I = 1/2$, natural abundances of 99.6 % and 0.4 %, and, in these states, sensitivities in comparison with $^{1}$H nuclei (1.0) of 1.0 x $10^{-3}$ and 3.8 x $10^{-6}$, respectively. Due to the low natural abundance of the $^{15}$N isotope, $^{15}$N solid-state NMR spectroscopic studies of catalytic systems require an isotopic enrichment. Because of the quadrupole moment of the $^{14}$N isotope of $Q = 2.04 \times 10^{-30}$ m$^2$, quadrupolar interactions are the dominating signal broadening mechanism for these nuclei. Both $^{14}$N and $^{15}$N nuclei have low resonance frequencies, which are often not in the range of standard solid-state NMR probes. In this case, a specific low-frequency NMR probe is required for $^{14}$N and $^{15}$N solid-state NMR investigations. For basic principles of solid-state NMR, see lectures "Solid-State NMR Spectroscopy" for Bachelor students or PhD seminars, accessible via the link "Lectures for Students".

In the research field of heterogeneous catalysis, the application **$^{14}$N solid-state NMR spectroscopy** is mainly restricted to studies of **nitrogen-containing structure**

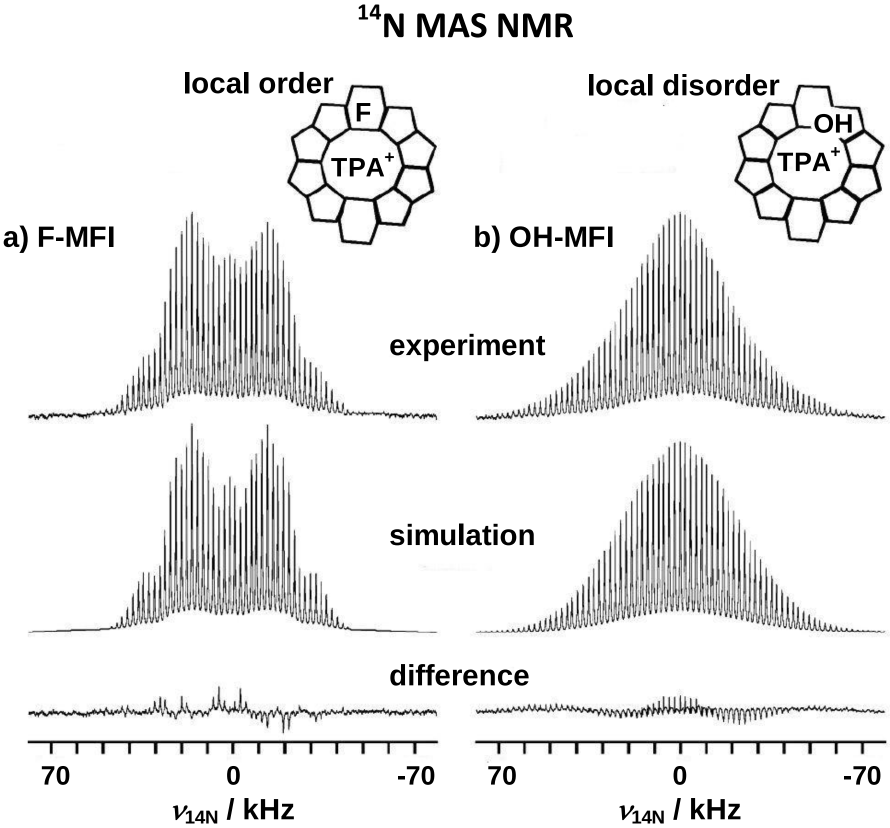

Fig. 1

**directing agents (SDA)** utilized in the synthesis of microporous zeolites [1-6]. Examples are investigations of tetrapropylammonium ($TPA^+$) [1-3, 6], tripropylethylammonium, ($TPEA^+$) [2, 6], butyltripropylammonium ($BTPA^+$) [2], and mixtures of tetraethylammonium ($TEA^+$) [4] and tetraethylphosphonium ($TEP^+$) [4] cations in MFI-type zeolites and tetraethylammonium ($TEA^+$) cations in $AlPO_4$-5 [5]. One of the aims of these $^{14}$N solid-state NMR studies was the determination of the order or disorder in the local structure of the nitrogen-containing SDAs.

**Fig. 1** shows $^{14}$N MAS NMR spectra of as-synthesized Silicalite-1, prepared via the fluoride route with TPABr and $NH_4F$ (F-MFI) and via the alkaline route with TPAOH (OH-MFI), and recorded at a Larmor frequency of $\nu_0$ = 43.3 MHz and with a MAS rate of $\nu_{\mathrm{rot}}$ = 2.0 kHz [1]. In the case of F-MFI, a single $^{14}$N MAS NMR signal with a well-defined spinning sideband (SSB) pattern occurs (**Fig. 1a**). The simulation of the SSB envelope led to a single $^{14}$N quadrupolar parameter set of $C_{\mathrm{Q}}$ = 52.8 kHz and $\eta_{\mathrm{Q}}$ = 0.3 [1]. In contrast to F-MFI, the $^{14}$N MAS NMR spectrum of OH-MFI is featureless (**Fig. 1b**). This kind of spectrum is the result of a distribution of $^{14}$N quadrupolar parameters. The mean $^{14}$N quadrupolar coupling constant was found to be $C_{\mathrm{Q,mean}} \cong$ 58 kHz, a value close to the value of $C_{\mathrm{Q}}$ = 52.8 kHz found for F-MFI. Therefore, the distribution of the $^{14}$N quadrupolar coupling constants for F-MFI cannot be due to SDA mobility. Otherwise, the $C_{\mathrm{Q,mean}}$ value would be significantly smaller. Since the $^{14}$N quadrupolar coupling constant depends on the local geometry of the $^{14}$N sites in the SDAs ($TPA^+$), i.e. mainly on the deviation of the C–N–C angles from the tetrahedral symmetry, the featureless $^{14}$N MAS NMR spectrum of OH-MFI in **Fig. 1b** hints to a local disorder. This local disorder corresponds to a distribution of the C–N–C angles and/or to a distribution of the compensating negative charges in the framework surrounding the $TPA^+$ cations [1].

**$^{15}$N solid-state NMR spectroscopy** is utilized in heterogeneous catalysis for the investigation of **surface sites by $^{15}$N-enriched probe molecule**s and of $^{15}$N-enriched reactants for the study of reaction mechanisms. However, because of the high costs of $^{15}$N-enriched chemicals, $^{15}$N solid-state NMR spectroscopy does not find a similar broad application like alternative resonances. For the characterization of surface sites on solid catalysts, $^{15}$N-enriched $N_2O$, $NH_3$, pyridine, and acetonitrile are used.

Before $^{15}$N chemical shift values of specific compounds can be considered, some remarks on discrepancies between different shift scales are necessary. According to suggestions of Refs. [7] and [8], $^{15}$N chemical shifts in **$^{15}$N liquid-state NMR** studies are referenced to **$\delta_{15N}$ = 0 ppm for liquid $^{15}NH_3$** and $\delta_{15N}$ = 380.6 ppm for neat $CH_3{}^{15}NO_2$. However, in most of the **$^{15}$N solid-state NMR** studies, $^{5}$N chemical shifts are referenced to **$\delta_{15N}$ = 0 ppm for neat $CH_3{}^{15}NO_2$** and $\delta_{15N}$ = -380.6 ppm for liquid $^{15}NH_3$. Therefore, the latter scale is also used for the subsequent presentation and discussion of literature data, sometimes slightly corrected by utilizing more recent values of Ref. [8]. Some groups use own scales, such as $\delta_{15N}$ = 0 ppm for solid $^{15}NH_4Cl$ [9, 10], $\delta_{15N}$ = 0 ppm for $^{15}NH_4NO_3$ solution [11], $\delta_{15N}$ = 0 ppm for solid $^{15}NH_4NO_3$ [12], $\delta_{15N}$ = 0 ppm for $NH_4{}^{15}NO_3$ [13] or $\delta_{15N}$ = 0 ppm for liquid $^{15}NH_3$ in $^{15}$N solid-state NMR spectroscopy [14-17]. In these cases, the corresponding $^{15}$N chemical shift values were transformed into the scale with $\delta_{15N}$ = 0 ppm for neat $CH_3{}^{15}NO_2$, excluding for the $\delta_{15N}$ values of $^{15}$N-acetonitrile in Ref. [13].

**Table 1** gives a survey on the application of probe molecules for the investigation of surface sites on various materials by $^{15}$N MAS NMR spectroscopy. In this connection must be mentioned, that the $^{15}$N chemical shift values in **Table 1** are often interpolated to an adsorbate loading of zero or determined at the lowest possible loading. The best loading is a 1 : 1 adsorption at the surface sites under study, which is much easier to control by $^{1}$H MAS NMR spectroscopy compared with $^{15}$N MAS NMR spectroscopy. Otherwise, a rapid exchange of adsorbed and gaseous probe molecules may occur, having a significant influence on the experimentally observed signal positions, already at room temperature.

| **Probe Molecules** | **Materials** | **Compounds / Sites** | **$\delta_{15}$/ppm** | **Refs.** |
|---|---|---|---|---|
| **terminale $^{15}$N in $^{15}N_2O$** | $^{15}N_2O$ | gaseous | -235.5 | [18] |
| | $\gamma$-$Al_2O_3$ | at LAS | -210 to -220 | [18], [19] |
| | Na-Y | at LAS | -228.8 | [18] |
| | deal. H-Y | at LAS | -226 to -220 | [20] |
| | Na-ZSM-5 | at LAS | -230 to -231 | [20], [21] |
| | H-ZSM-5 | at LAS | -221 to -212 | [20], [21] |
| **$^{15}NH_3$** | $^{15}NH_3$ | gaseous | -399.9 | [22] |
| | $^{15}NH_3$ | liquid | -380.6 | [8] |
| | $^{15}NH_3$ | physisorbed | -364.0 | [9] |
| | $^{15}NH_4{}^{+}NO_3$ | 1 M solution | -360.0 | [8] |

| | | | | |
|---|---|---|---|---|
| | $^{15}NH_4^+NO_3$ | powder | -358.6 | [8] |
| | $V_2O_5/TiO_2$ | strongly adsorbed | -368.9 | [11] |
| | zeolite Na,K-A (site loading ≅ 1 : 1) | site I | -386.4 | [23] |
| | | site II | -389.1 | [23] |
| | | site III | -385.1 | [23] |
| | | site IV | -390.6 | [23] |
| | zeolites Na-A, Na-X, Na-Y (extrapolated to small loadings) | | ca. -395 | [22] |
| | $\gamma$-$Al_2O_3$, USY | at $Al^{IV}$ | -365.1±0.5 | [9] |
| | | at $Al^{V}$ | -373.6±1.5 | [9] |
| | zeolite 88H-Y (site loading ≅ 1 : 1.9 to 1 : 4.4) | at Si(OH)Al | -361 | [22] |
| **$^{15}$N-pyridine** | SBA-15 | bulk pyridine | -65 to -64 | [10], [16] |
| | SBA-15 | at SiOH | -90 to -83 | [10] |
| | titanosilicalite-1 | at SiOH | -89 | [17] |
| | titanosilicalite-1 | at Ti | -100 | [17] |
| | $AlF_x(OH)_{3-x}$ | at LAS | -123 to -116 | [24] |
| | silica-alumina | at LAS | -117 | [14], [15] |
| | Sn/MFI, Sn/MCM-41 | at LAS | -119 | [16] |
| | Sn/Beta | at LAS | -121 to -116 | [16] |
| | $AlCl_xF_{3-x}$ | at LAS | -125.5 -138.7 | [25] |
| | [Al]SBA-15 | at LAS | -141 | [10] |
| | $(SG)_nAlCl_2$ | at LAS | -145 | [26] |
| | F/Beta | at BAS | -169 | [16] |
| | titanosilicalite-1 | at BAS | -169 | [17] |
| | high-surface-$AlF_3$ | at BAS | -171 | [25] |
| | [Al]SBA-15 | at BAS | -174 | [10] |
| | H-ZSM-5 | at BAS | -176 | [26] |
| | $AlF_x(OH)_{3-x}$ | at BAS | -178 | [24] |
| | $AlCl_xF_{3-x}$ | at BAS | -178 | [25] |
| | silica-alumina | at BAS | -183 | [14], [15] |
| | $\gamma$-$Al_2O_3$ | at BAS | -185 | [12] |
| | H-Mordenite | at BAS | -188 | [12] |

| | | | | |
|---|---|---|---|---|
| | (silica gel)$_n$AlCl$_2$ | at BAS | -188 | [26] |
| **$^{15}$N-acetonitrile** | H-ZSM-5 | physisorbed | -243.4 | [13] |
| | H-ZSM-5 | at LAS | -253.9 | [13] |
| | H-ZSM-5 | at BAS | -269.2 | [13] |

LAS: Lewis acid sites
BAS: Broensted acid sites

**Table 1**

In addition to the experimental $^{15}$N solid-state NMR studies of probe molecules, summarized in **Table 1**, quantum-chemical studies of $^{15}$N-pyridine on metal-doped amorphous silicates [27] and $^{15}$N-acetonitrile on various solid acids [28, 29] were performed.

Examples for **$^{15}$N solid-state NMR spectroscopic studies of reaction mechanisms** in the field of heterogeneous catalysis are the conversion of $^{15}NH_3$ and methanol to methylamines on zeolites H-RHO and H-SAPO-34 [30] or the conversion of $^{15}$NO with different reactants on various ZSM-5 zeolites [31-33]. The reaction, which was most often studied by $^{15}$N solid-state NMR spectroscopy, is the **Beckmann rearrangement of different oximes** on solid catalysts [34-38]. In chemical industry, ε-caprolactam is an important reactant for the production of Polyamid 6 (Perlon). To replace the conventional method for synthesizing ε-caprolactam in concentrated sulfuric acid or oleum, the vapor-phase **Beckmann rearrangement of cyclohexanone oxime** to ε-caprolactam on solid catalysts is interesting as an environmentally benign process.

**Scheme 1** gives an overview on the suggested **reaction mechanism** as well as experimentally observed (without parenthesis [35, 36]) and calculated (in parenthesis [39]) $^{15}$N chemical shifts [35]. The first steps of the Beckmann rearrangement of cyclohexanone oxime on zeolites are the adsorption of the reactants via hydrogen bonding at SiOH groups in Silicalite-1 (**A**) or the N-protonation of the reactant by hydroxyl groups in zeolites H-ZSM-5 and H-[B]ZSM-5 (**B**). On strong acid sites, a 1,2-H shift leading to O-protonated cyclohexanone oxime **C** is followed by the formation of carbenium ions **D** as intermediates. A more stable state of this intermediate is the nitrilium ion **E**. The calculated $^{15}$N chemical shift of $\delta_{15N}$ = -224 ppm for this intermediate indicates that species **E** may be responsible for $^{15}$N NMR signals at $\delta_{15N}$

= -237 ppm. The further conversion of species **E**, which should be accompanied with a decrease of the signal at $\delta_{15N}$ = -237 ppm, leads to the formation of non-protonated and protonated $\varepsilon$-caprolactam (**F** and **G**, respectively) causing $^{15}$N NMR signals at $\delta_{15N}$ = -260 ppm and $\delta_{15N}$ = -347 ppm, respectively [36].

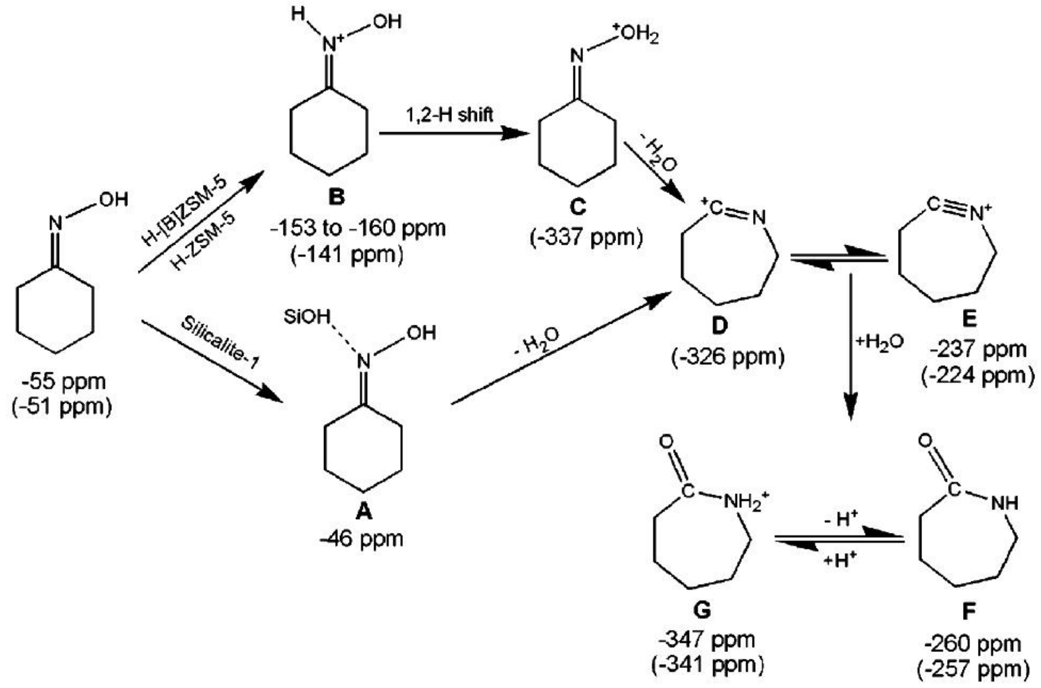

**Scheme 1**

The *in situ* $^{15}$N CPMAS NMR studies shown in **Fig. 2** were perfomed under batch conditions (see Section “method 29”) and focused on the conversion of $^{15}$N-cyclohexanone oxime (educt, signal $\delta_{15N}$ = -55 to 45 ppm) on the zeolites Silicalite-1, H-ZSM-5, and H-[B]ZSM-5 by stepwise heating of the physical mixtures of the reactant and the calcined zeolite catalysts at temperatures between $T$ = 423 and 523 K [34]. According to **Fig. 2a**, the Beckmann rearrangement on Silicalite-1 starts at about $T$ = 473 K, which is indicated by new signals at $\delta_{15N}$ = -237 ppm (**E**), -260 (**F**), and -376 ppm. After raising the reaction temperature to $T$ = 498 and 523 K (**Figs. 2b and 2c**), the spectra consist of a single signal at $\delta_{15N}$ = -260 ppm (**F**) due to the final product of the Beckmann rearrangement. The signal at $\delta_{15N}$ = -376 ppm is a hint for the formation of an amine as a byproduct [34].

The Beckmann rearrangement of $^{15}$N-cyclohexanone oxime on zeolite H-ZSM-5 starts at about $T$ = 423 K (**Fig. 2d**). In addition to the $^{15}$N CPMAS NMR signal of protonated and non-interacting $^{15}$N-cyclohexanone oxime at $\delta_{15N}$ = -160 ppm (**B**) and

$\delta_{15N}$ = -55 ppm (**educt**), respectively, a signal at $\delta_{15N}$ = -347 ppm (**G**) due to protonated ε-caprolactam occurs. The spectrum in **Fig. 2d** is dominated by a signal at $\delta_{15N}$ = -237 ppm (**E**), which already appeared in the spectrum of Silicalite-1 heated at $T$ = 473 K (**Fig. 2a**) [34].

A more complicated situation occurs for the Beckmann rearrangement of $^{15}$N-cyclohexanone oxime on zeolite H-[B]ZSM-5 (**Figs. 2g to 2i**). In addition to the $^{15}$N CPMAS NMR signals observed for the conversion of $^{15}$N-cyclohexanone oxime on Silicalite-1 and H-ZSM-5, signals of byproducts occur at $\delta_{15N}$ = -199 ppm (protonated 5-cyano-1-pentene), -275 ppm (hydroxylamine), and -364 ppm (ε-aminocaproic acid) [34]. These byproducts are the reason for the loss of the ε-caprolactam selectivity of zeolite H-[B]ZSM-5 after a short time on stream in comparison with Silicalite-1 as described in Ref. [40]. For further information and experimental details, see Section "method 29".

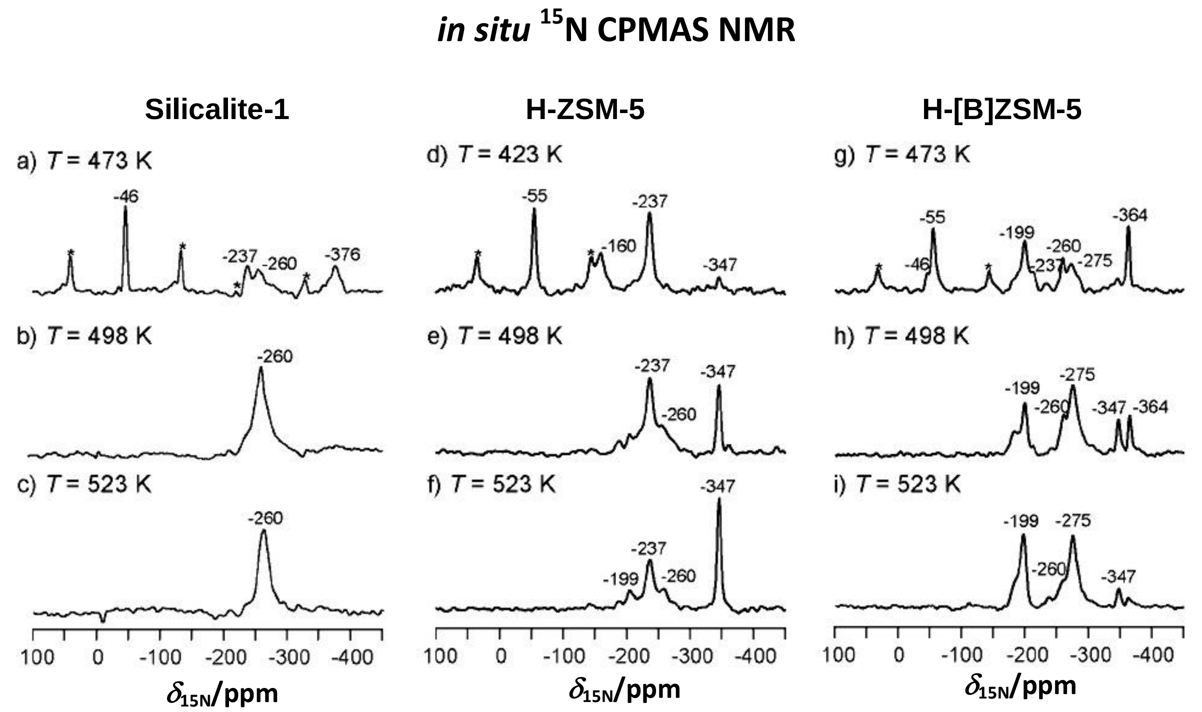

Fig. 2

***Catalyst preparation:*** The samples used for the $^{14}$N MAS NMR studies of SDAs were in the as-synthesized state. The post-treatment of the F-MFI material was done in an autoclave ($T$ = 448 K, 4 days) using a 0.07 wt.-% $NH_4OH$ solution [1]. The preparation procedures of the sample materials utilized for $^{15}$N solid-state NMR studies of $^{15}$N-enriched probe molecules, summarized in **Table 1**, are very different and described in the corresponding references. For the *in situ* solid-state NMR studies of the Beckmann rearrangement of $^{15}$N-cyclohexanone oxime, the catalysts were dehydrated inside a “sample tube system 1“ at “vacuum line 1“, both accessible via link “*In Situ* Solid-State NMR Techniques”. The dehydration starts with an evacuation at room temperature for ca. 10 minutes, followed by a temperature ramp from room temperature to $T$ = 393 K within 2 hours. At this temperature, the sample was dehydrated for 2 hours. Subsequently, the temperature was increased up to $T$ = 723 K within 3 hours and the sample was evacuated at this temperature for 12 hours. After this treatment, the sample tube system was closed via the vacuum valve and disconnected from the vacuum line (after this line was ventilated with air). Mixtures of $^{15}$N-cyclohexanone oxime and dehydrated catalysts were prepared as follows. First, 20 mg of $^{15}$N-cyclohexanone oxime was evacuated at room temperature and mixed with ca. 300 mg of dehydrated zeolite in a mini glove box (see Section “mini glove box”, accessible via link “*In Situ* Solid-State NMR Techniques”), purged with dry nitrogen gas. Subsequently, the catalyst loaded with $^{15}$N-cyclohexanone oxime was filled into an MAS NMR glass ampoule (see Section “sample tube system 4”, accessible via link “*In Situ* Solid-State NMR Techniques”), evacuated at room temperature at “vacuum line 2” (see Section “vacuum line 2”, accessible via link “*In Situ* Solid-State NMR Techniques”), and, finally, sealed.

***$^{14/15}$N solid-state NMR studies:*** The$^{14}$N MAS NMR spectra shown in **Fig. 1** were recorded at a Larmor frequency of $\nu_0$ = 43.3 MHz, with a $\pi/4$ pulse excitation, and with a MAS rate of $\nu_{\rm rot}$ = 2.0 kHz utilizing 9.5 mm rotors. With a repetition time of 0.5 s, recording of the spectra in **Fig. 1a** (46.000 scans) and **Fig. 1b** (98.000 scans) required ca. 6 h and 14 h, respectively [1].

The *in situ* $^{15}$N CPMAS NMR spectra of the catalyst loaded with reactants in **Fig. 2** were recorded at a Bruker MSL 400WB spectrometer at a resonance frequency of $\nu_0$ = 40.53 MHz and using a 7 mm Bruker MAS NMR probe with sample spinning rates of $\nu_{\rm rot}$ = 3.5 to 4.7 kHz. The CPMAS NMR spectra were obtained with a contact time of $\tau$ = 5 ms and a recycle delay of 2 s. The $^{15}$N CPMAS NMR spectra were referenced to nitromethane ($\delta_{15N}$ = 0.0 ppm).

***References:***

[1] E. Dib, T. Mineva, P. Gaveau, B. Alonso, *$^{14}$N solid-state NMR: A sensitive probe of the local order in zeolites,* Phys. Chem. Chem. Phys. 15 (2013) 18349-18352, DOI: 10.1039/c3cp51845k.

[2] E. Dib, A. Gimenez, T. Mineva, B. Alonso, *Preferential orientations of structure directing agents in zeolites*, Dalton Trans. 44 (2015) 16680-16683, DOI: 10.1039/C5DT02558C.

[3] E. Dib, T. Mineva, P. Gaveau, E. Veron, V. Sarou-Kanian, F. Fayon, B. Alonso, *Probing disorder in Al-ZSM-5 zeolites by $^{14}$N NMR spectroscopy*, J. Phys. Chem. C 121 (2017) 15831-15841, DOI: 10.1021/acs.jpcc.7b04861.

[4] J. Martinez-Ortigosa, J. Simancas, J.A. Vidal-Moya, P. Gaveau, F. Rey, B. Alonso, T. Blasco, *Host−guest and guest−guest interactions of P- and N-containing structure directing agents entrapped inside MFI-type zeolite by multinuclear NMR spectroscopy*, J. Phys. Chem. C 123 (2019) 22324-22334, DOI: 10.1021/acs.jpcc.9b05689.

[5] J. Xu, Y. Liu, Y. Huang, *Ultrafast crystallization of $AlPO_4$-5 molecular sieve in a deep eutectic solvent*, J. Phys. Chem. C 125 (2021) 8876-8889, DOI: 10.1021/acs.jpcc.1c01690.

[6] M. Fabbiani, S. Al-Nahari, L. Piveteau, E. Dib, V. Veremeienko, A. Gaje, D.G. Dumitrescu, P. Gaveau, T. Mineva, D. Massiot, A. Lee, J. Haines, B. Alonso, *Host-guest silicalite-1 zeolites: Correlated disorder and phase transition inhibition by a small guest modification*, Chem. Mater. 34 (2022) 366-387, DOI: 10.1021/acs.chemmater.1c03721.

[7] J.L. Markley, A. Bax, Y. Arata, C.W. Hilbers, R. Kaptein, B.D. Sykes, P.E. Wright, K. Wuethrich, *Recommendations for the presentation of NMR structures of proteins and nucleic acids, IUPAC-IUBMB-IUPAB interunion task group on the standardization of data bases of protein and nucleic acid structures determined by NMR spectroscopy*, Eur. J. Biochem. 256 (1998) 1-15, DOI: 10.1046/j.1432-1327.1998.2560001.x.

[8] P. Bertanin, J. Raya, B. Bechinger, *$^{15}$N chemical shift referencing in solid state NMR*, Solid State Nucl. Magn. Reson. 61-62 (2014) 15-18, DOI: 10.1016/j.ssnmr.2014.03.003.

[9] D. Coster, A.L. Blumenfeld, J.J. Fripiat, *Lewis acid sites and surface aluminum in aluminas and zeolites: A high-resolution NMR study*, J. Phys. Chem. 98 (1994) 6201-6211, DOI: 10.1021/j100075a024.

[10] A.A. Gurinov, Y.A. Rozhkova, A. Zukal, J. Cejka, I.G. Shenderovich, *Mutable Lewis and Broensted acidity of aluminated SBA-15 as revealed by NMR of*

*adsorbed pyridine-15N*, Langmuir 27 (2011) 12115-12123, DOI: 10.1021/la2017566.

[11] S. Hu, T.M. Apple, *$^{15}$N NMR study of the adsorption of NO and $NH_3$ on titania-supported vanadia catalysts*, J. Catal. 158 (1996) 199-204, DOI: 10.1006/jcat.1996.0019.

[12] J.A. Ripmeester, *Surface acid site characterization by means of CP/MAS nitrogen-15 NMR*, J. Am. Chem. Soc. 105 (1983) 2925-2927, DOI: 10.1021/ja00347a083.

[13] F. C. Feyen, P. K. Burkert, *Nitrogen-15 and boron-11 NMR spectroscopy of the system acetonitrile / H-ZSM-5*, Z. Naturforsch. B 50 (1995) 1753-1758, DOI: 10.1515/znb-1995-1124.

[14] G.E. Maciel, J.F. Haw, I.-S. Chuang, B.L. Hawkins, T.A. Early, D.R. McKay, L. Petrakis, *NMR studies of pyridine on silica-alumina*, J. Am. Chem. Soc. 105 (1983) 5529-5535, DOI: 10.1021/ja00355a001.

[15] J.F. Haw, I.-S. Chuang, B.L. Hawkins, G.E. Maciel, *Surface titration of silica-alumina monitored by nitrogen-15 NMR with cross polarization and magic-angle spinning*, J. Am. Chem. Soc. 105 (1983) 7206-7207, DOI: 10.1021/ja00362a051.

[16] W.R. Gunther, V.K. Michaelis, R.G. Griffin, Y. Roman-Leshkov, *Interrogating the Lewis acidity of metal sites in Beta zeolites with $^{15}$N pyridine adsorption coupled with MAS NMR spectroscopy*, J. Phys. Chem. C 120 (2016) 28533-28544, DOI: 10.1021/acs.jpcc.6b07811.

[17] L. Laetsch, C.J. Kaul, A.V. Yakimov, R. McEntee,T. De Baerdemaeker, A.-N. Parvulescu, K. Seidel, J.H. Teles, C. Copéret, *Nature of reactive sites in TS-1 from $^{15}$N solid-state NMR and Ti K-edge X-ray absorption spectroscopic signatures upon pyridine adsorption*, J. Am. Chem. Soc. 146 (2024) 29675-29683, DOI: 10.1021/jacs.4c10604.

[18] V.M. Mastikhin, I.L. Mudrakovsky, S.V. Filimonova, *Probing the Lewis acidity of heterogeneous catalysts by $^{15}$N NMR of adsorbed $N_2O$*, Chem. Phys. Lett. 149 (1988) 175-179, DOI: 10.1016/0009-2614(88)87217-8.

[19] S.V. Filimonova, V.M. Mastikhin, *Probing the surface acidity of modified $\gamma$-alumina with $^{1}$H and $^{15}$N high-resolution solid state NMR spectroscopy*, React. Kinet. Catal. Lett. 65 (1998) 131-138, DOI: 10.1007/BF02475326.

[20] V.M. Mastikhin, I.L. Mudrakovsky, S.V. Filimonova, *Testing of the Lewis acidity of H-Y and HZSM-5 zeolites with $^{15}$N n.m.r. of adsorbed $N_2O$*, Zeolites 10 (1990) 593-597, DOI: 10.1016/S0144-2449(05)80318-5.

[21] V. M. Mastikhin, S. V. Filimonova, I. L. Mudrakovsky, V. N. Romannikov, *Role of iron impurities in formation of electron-accepting sites in H-ZSM-5 zeolites: $^{15}$N nuclear magnetic resonance and $^{15}$N nuclear magnetic relaxation*

*of adsorbed $N_2$ and $N_2O$*, J. Chem. Soc., Faraday Trans. 87 (1991) 2247-2252, DOI: 10.1039/ft9918702247.

[22] D. Michel, A. Germanus, H. Pfeifer, *Nitrogen-15 nuclear magnetic resonance spectroscopy of adsorbed molecules*, J. Chem. Soc., Faraday Trans. 78 (1982) 237-254, DOI: 10.1039/f19827800237.

[23] G.P. Holland, B.R. Cherry, T.M. Alam, *$^{15}N$ solid-state NMR characterization of ammonia adsorption environments in 3A zeolite molecular sieves*, J. Phys. Chem. B 108 (2004) 16420-16426, DOI: 10.1021/jp047884j.

[24] F. Hemmann, G. Scholz, K. Scheurell, E. Kemnitz, C. Jaeger, *Time-optimized $^{15}N$ qNMR determination of Lewis and Broensted site concentrations and chemical bonding of pyridine at Broensted sites in amorphous aluminum hydroxide fluoride*, J. Phys. Chem. C 116 (2012) 10580-10585, DOI: 10.1021/jp212045w.

[25] B. Calvo, C.P. Marshall, T. Krahl, J. Kroehnert, A. Trunschke, G. Scholz, T. Braun, E. Kemnitz, *Comparative study of the strongest solid Lewis acids known: ACF and HS-$AlF_3$*, Dalton Trans. 47 (2018) 16461-16473, DOI: 10.1039/c8dt03279c.

[26] T. Xu, N. Kob, R.S. Drago, J.B. Nicholas, J.F. Haw, *A solid acid catalyst at the threshold of superacid strength: NMR, calorimetry, and density functional theory studies of silica-supported aluminum chloride*, J. Am. Chem. Soc. 119 (1997) 12231-12239, DOI: 10.1021/ja970850n.

[27] A. Jystad, H. Leblanc, M. Caricato, *Surface acidity characterization of metal-doped amorphous silicates via Py-FTIR and $^{15}N$ NMR simulations*, J. Phys. Chem. C 124 (2020) 15231-15240, DOI: 10.1021/acs.jpcc.0c03292.

[28] A. Simperler, R.G. Bell, M.W. Anderson, *Probing the acid strength of Broensted acidic zeolites with acetonitrile: Quantum chemical calculation of $^{1}H$, $^{15}N$, and $^{13}C$ NMR shift parameters*, J. Phys. Chem. B 108 (2004) 7142-7151, DOI: 10.1021/jp035674l.

[29] D. Yi, H. Zhang, Z. Deng, *$^{1}H$ and $^{15}N$ chemical shifts of adsorbed acetonitrile as measures to probe the Broensted acid strength of solid acids: A DFT study*, J. Mol. Catal. A: Chemical 326 (2010) 88-93, DOI: 10.1016/j.molcata.2010.04.012.

[30] A. Thursfield, M.W. Anderson, J. Dwyer, G.J. Hutchings, D. Lee, *$^{13}C$ and $^{15}N$ solid-state MAS NMR study of the conversion of methanol and ammonia over H-RHO and H-SAPO-34 microporous catalysts*, J. Chem. Soc., Faraday Trans. 94 (1998) 1119-1122, DOI: 10.1039/a709294f.

[31] V.M. Mastikhin, S.V. Filimonova, *$^{15}N$ nuclear magnetic resonance studies of the NO-$O_2$-$NH_3$ reaction over ZSM-5 zeolites*, J. Chem. Soc., Faraday Trans. 88 (1992) 1473-1476, DOI: 10.1039/FT9928801473.

[32] S.V. Filimonova, V.M. Mastikhin, *$^{15}$N NMR studies of the NO-$NH_3$-$O_2$ reaction over ZSM-5 type zeolites and vanadia supported catalysts*, React. Kinet. Catal. Lett. 54 (1995) 419-426, DOI: 10.1007/BF02071035.

[33] J. Wu, S.C. Larsen*, $^{15}$N solid state NMR study of the reactions of propane or propene,$^{15}$NO and oxygen on Na-, H-, and CuZSM*-5, Catal. Lett. 70 (2000) 43-50, DOI: 10.1023/A:1019091906005.

[34] V.R. Reddy Marthala, Y. Jiang, J. Huang, W. Wang, R. Glaser, M. Hunger, *Beckmann rearrangement of $^{15}$N-cyclohexanone oxime on zeolites silicalite-1, H-ZSM-5, and H-[B]ZSM-5 studied by solid-state NMR spectroscopy*, J. Am. Chem. Soc. 128 (2006) 14812-14813, DOI: 10.1021/ja066392c.

[35] A.B. Fernández, I. Lezcano-Gonzalez, M. Boronat, T. Blasco, A. Corma, *NMR spectroscopy and theoretical calculations demonstrate the nature and location of active sites for the Beckmann rearrangement reaction in microporous materials*, J. Catal. 249 (2007) 116-119, DOI: 10.1016/j.jcat.2007.03.030.

[36] V.R. Reddy Marthala, S. Rabl, J. Huang, B. Thomas, M. Hunger, *In situ solid-state NMR investigations of the vapor-phase Beckmann rearrangement of $^{15}$N-cyclohexanone oxime on MFI-type zeolites and mesoporous SBA-15 materials in the absence and presence of the additive $^{13}$C-methanol*, J. Catal. 257 (2008) 134-141, DOI: 10.1016/j.jcat.2008.04.014

[37] A.B. Fernandez, I. Lezcano-Gonzalez, M. Boronat, T. Blasco, A. Corma, *Study of the Beckmann rearrangement of acetophenone oxime over porous solids by means of solid state NMR spectroscopy*, Phys. Chem. Chem. Phys. 11 (2009) 5134-5141, DOI: 10.1039/b816276j.

[38] T. Blasco, A. Corma, S. Iborra, I. Lezcano-González, R. Montón, *In situ multinuclear solid-state NMR spectroscopy study of Beckmann rearrangement of cyclododecanone oxime in ionic liquids: The nature of catalytic sites*, J. Catal. 275 (2010) 78-83, DOI: 10.1016/j.jcat.2010.07.016.

[39] NNMR Predictor & dB 9.0, Advanced Chemistry Development, Inc.: Toronto, Ontario, Canada.

[40] L. Forni, E. Patriachi, G. Fornasari, F. Trifiro, A. Katovic, G. Giordano, J.B. Nagy, *Synthesis of porous catalysts for Beckmann rearrangement of oximes*, Stud. Surf. Sci. Catal. 155 (2005) 281-290, DOI: 10.1016/S0167-2991(05)80156-9.